Directed Evolution of Epoxide Hydrolase from *A. radiobacter* toward Higher Enantioselectivity by Error-Prone PCR and DNA Shuffling

Bert van Loo,[1] Jeffrey H. Lutje Spelberg,[1]
Jaap Kingma,[1] Theo Sonke,[2] Marcel G. Wubbolts,[2]
and Dick B. Janssen[1],*
[1]Biochemical Laboratory
Groningen Biomolecular Sciences and
Biotechnology Institute
University of Groningen
Nijenborgh 4
9747 AG Groningen
[2]DSM Pharma Chemicals
Advanced Synthesis, Catalysis & Development
P.O. Box 18
6160 MD Geleen
The Netherlands

Summary

The enantioselectivity of epoxide hydrolase from *Agrobacterium radiobacter* (EchA) was improved using error-prone PCR and DNA shuffling. An agar plate assay was used to screen the mutant libraries for activity. Screening for improved enantioselectivity was subsequently done by spectrophotometric progress curve analysis of the conversion of *para*-nitrophenyl glycidyl ether (pNPGE). Kinetic resolutions showed that eight mutants were obtained with up to 13-fold improved enantioselectivity toward pNPGE and at least three other epoxides. The large enhancements in enantioselectivity toward epichlorohydrin and 1,2-epoxyhexane indicated that pNPGE acts as an epoxyalkane mimic. Active site mutations were found in all shuffled mutants, which can be explained by an interaction of the affected amino acid with the epoxide oxygen or the hydrophobic moiety of the substrate. Several mutations in the shuffled mutants had additive effects.

Introduction

Epoxide hydrolases (E.C. 3.3.2.3) catalyze the net addition of a water molecule to an epoxide, resulting in a vicinal diol as the sole product. So far, all epoxide hydrolases for which the gene has been cloned, except for one [1], are members of the α/β-hydrolase fold family. These enzymes share a main domain consisting of a central β sheet surrounded by α helices, with a variable cap domain sitting on top [2]. The active site of epoxide hydrolases is located at the interface of the main domain and the cap domain and contains an Asp-His-Asp catalytic triad. This catalytic triad is conserved among epoxide hydrolases and haloalkane dehalogenases [3]. The active site of epoxide hydrolase further contains two tyrosines located in the cap domain, which are involved in substrate binding and assist in the ring opening of the epoxide by acting as proton donor to the epoxide oxygen [4–6].

*Correspondence: d.b.janssen@chem.rug.nl

Chiral epoxides and diols are important building blocks for the preparation of enantiopure pharmaceuticals and other fine chemicals. For example, styrene oxide derivatives (epoxides **1–3**, Figure 1) and phenyl glycidyl ethers (**4** and **5**) can be used in the synthesis of β-adrenergic agonists by ring opening of the chiral epoxide with an amine [7–9]. Epichlorohydrin (**6**, Figure 1) can be used in the synthesis of food additives [10], antibacterial agents [11], and pharmaceuticals [12]. In these examples, the epoxide is mainly used in a nucleophilic ring-opening reaction that occurs with retention of configuration around the chiral center of the epoxide. It is therefore important to start the conversion with enantiopure epoxide. Existing methods for preparing enantiopure epoxides and vicinal diols include asymmetric synthesis, which can be done by epoxidation of a carbon-carbon double bond using chiral metalosalen complexes [13] or monooxygenases [14], and kinetic resolution of a racemic epoxide, using a Jacobsen catalyst [15] or an epoxide hydrolase [16].

Several epoxide hydrolases are enantioselective and have been tested in kinetic resolutions to obtain an enantiopure epoxide and an optically active diol with the opposite stereochemistry at the chiral center [16]. The yield of the remaining substrate and the enantiopurity of the diol are often not very high due to the low enantioselectivity of the enzyme. Therefore, it is desirable to improve the enantioselectivity of epoxide hydrolases, which so far has been described for the enzymes from *Agrobacterium radiobacter* [5, 17] and *Aspergillus niger* [18]. With *A. radiobacter* epoxide hydrolase, rational design using site-directed mutagenesis of the ring-opening tyrosines resulted in 2- to 5-fold improved enantioselectivity toward a number of aromatic epoxides [5, 17, 19]. The enantioselectivity of the epoxide hydrolase from *A. niger* toward phenyl glycidyl ether was recently 2-fold improved by random mutagenesis [18], but the enantioselectivity of the best mutant (E = 10.8) was not higher than that of the *A. radiobacter* wild-type enzyme (E = 11) [17].

In this paper, we report the use of directed evolution for improving the enantioselectivity of the epoxide hydrolase from *A. radiobacter* (EchA). Since this approach uses large libraries of mutants, rapid methods for screening the activity and enantioselectivity are desirable. An agar plate assay for epoxide hydrolase activity, which uses the oxidative power of *Escherichia coli* toward vicinal diols that are produced by epoxide hydrolysis, was developed. Screening for improved enantioselectivity of mutants was conveniently done using progress curve analysis of the conversion of a colorimetric substrate. The epoxide hydrolase from *A. radiobacter* has been well characterized, both structurally and kinetically [20, 21], and various active site mutants have been described earlier [5, 6, 17, 19]. After error-prone PCR and recombination of the beneficial mutations by DNA shuffling [22], mutants were obtained with 2- to 20-fold improved enantioselectivity with various epoxide substrates.
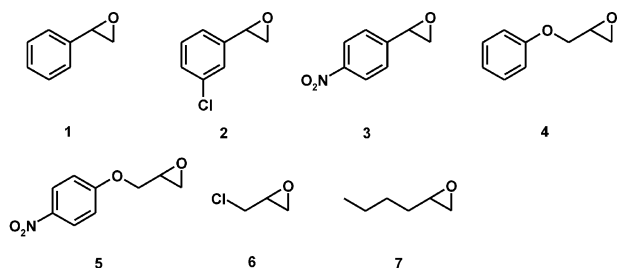
Figure 1. Epoxide Substrates Used in This Study

1, styrene oxide; 2, *meta*-chlorostyrene oxide; 3, *para*-nitrostyrene oxide; 4, phenyl glycidyl ether; 5, *para*-nitrophenyl glycidyl ether; 6, epichlorohydrin; 7, 1,2-epoxyhexane.

Results

Error-Prone PCR Mutagenesis of EchA

A library of random mutants of EchA was generated using error-prone PCR. The conditions used in the PCR reaction yielded 5–7 bp substitutions per gene, calculated from randomly picked mutants that were se-

quenced. This corresponds to an average of 2–3 amino acid substitutions per mutant. The library of mutant genes was cloned and expressed in *E. coli*. For expression, we used the pBAD system with which expression can be dosed by adjusting the L-arabinose concentration and which appeared much more stable than the pGEF expression system that we [23] and others [18] used earlier.

The resulting library of around 40,000 colonies was screened for activity toward 1,2-epoxybutane using an agar plate assay with safranin O as an indicator of membrane potential (Figure 2A). This assay is based on the oxidation by *E. coli* of diols that are produced by epoxide hydrolysis. NADH that is thereby generated causes an increase of the membrane potential due to the action of the respiratory chain. The stronger proton gradient that is generated enhances the uptake of safranin O and its accumulation inside the cell, as was observed for mitochondria [24]. *E. coli* colonies that possessed epoxide hydrolase activity obtained a rather uniform pink color due to accumulation of the dye, whereas inactive colonies had an uncolored outer ring. The test was verified with wild-type enzyme and various active and inac-
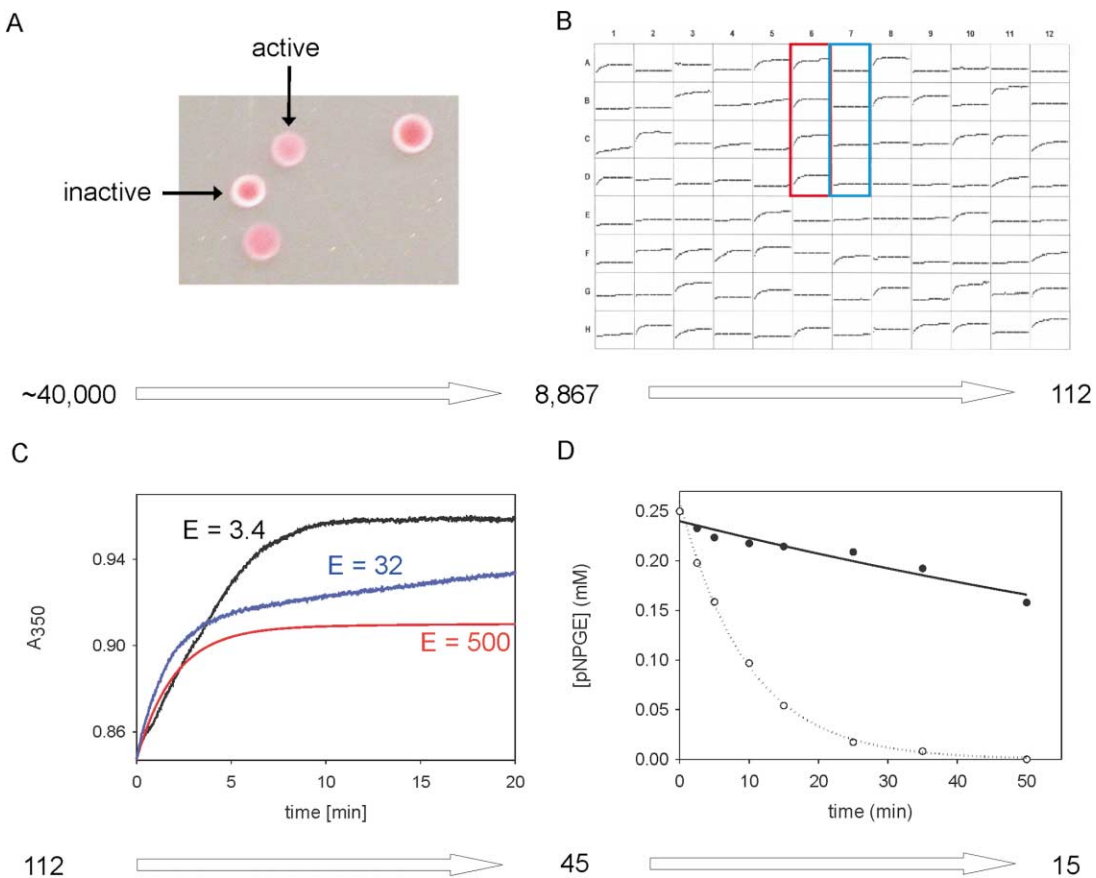

Figure 2. Screening Procedure for Enhanced Enantioselectivity

(A) Activity screening of colonies using safranin O indicator plates.
(B) UV/VIS progress curves of pNPGE (5) conversion with whole cells in 96-well plates. Wells A6–D6 (red border) and A7–D7 (blue border) represent wild-type controls and blank incubations, respectively.
(C) UV/VIS progress curves of pNPGE conversion by cell-free extract. The curve with E = 3.4 was obtained with wild-type EchA. The curve with E = 32 was obtained with mutant S4 (Table 1). The curve with E = 500 is a simulation that indicates the curve in case of perfect enantioselectivity.
(D) Chiral HPLC analysis of a kinetic resolution of 0.5 mM racemic pNPGE. The example is mutant M5. (●), (*R*)-pNPGE; (○), (*S*)-pNPGE.

tive mutants that were available from previous studies [5, 25]. By using the activity prescreening, the more time-consuming screening for enantioselectivity could be restricted to mutants that are active with at least one enantiomer of the racemic substrate. In this way, 78% of the mutants turned out to be inactive. These mutants were excluded from the next step. The activity screening yielded 8867 active clones (22%), which were grown and stored in microtiter plates.

The library of active clones was screened for improved enantioselectivity by following the time course of the conversion of a racemic mixture of *para*-nitrophenyl glycidyl ether (pNPGE, epoxide **5** in Figure 1). Conversion was monitored at 350 nm for 1 hr in a microtiter plate reader (Figure 2B). Around 70% of the selected mutants were active with pNPGE. The progress curves were subsequently analyzed as described under Experimental Procedures. An increase in enantioselectivity was indicated by the presence of a bend in the progress curve, which is not observed with the wild-type enzyme. Mutants with low activity and poor enantioselectivity were discarded. This way, 112 mutants in which the enantioselectivity was potentially increased were selected. Most of these mutants showed incomplete conversion or a clearly biphasic conversion of racemic substrate. The selected mutants were grown in a larger volume, and subsequently crude extracts of the cells were used for recording spectrophotometric progress curves of pNPGE hydrolysis with a normal cuvette. The curves were again inspected for the presence of a second kinetic phase (Figure 2C), which yielded 45 mutants that were selected for precise determination of their E-value in a kinetic resolution of pNPGE. The progress curve data were fitted according to competitive Michaelis-Menten kinetics in a similar way as described before [26] (Figure 2D). This does not result in unique solutions for the k_{cat} and K_m values for both enantiomers, but the ratio between the k_{cat}/K_m values, which is the E-value, is accurately obtained. Of the 45 mutants tested, 15 mutants showed a 1.5- to 4-fold improved enantioselectivity toward pNPGE as compared to wild-type EchA (Table 1).

Sequence analysis of the 15 improved mutants showed that the number of amino acid substitutions varied from 1 to 6 per mutant, with a total of 34 mutated positions (Table 1). Using the X-ray structure of EchA (1EHY) [21], it appeared that 21 of the mutated positions were located in the main domain, which contains 204 amino acids (residues 1–134 and 225–294). From these 21 mutated positions, 13 were located at the top near the interface with the cap domain, and 5 were located at the bottom (Figure 3A). Only 3 mutated residues were located in the middle part of helices of the main domain (Figure 3A). The central part of the β sheet of the main domain was completely free of mutations.

In the cap domain, 13 positions out of 90 (residues 135–224) were mutated. These mutations were distributed all over the cap domain (Figure 3A).

Shuffling Mutants with Enhanced Enantioselectivity

In order to recombine the beneficial mutations generated by the error-prone PCR, the genes of the 15 im-

Table 1. Enantioselectivities toward pNPGE (5) of EchA Mutants

Mutant	Mutations[a]	E-value[b]
M1	A110G, K126E, E192G	4.3
M2	**Y215F**	9.1
M3	L35M, H198L, C202S, H209R, D287E	12.0
M4	V112I, **Y215F**	11.0
M5	T31P, A110G, **Y152F**	14.0
M6	**F108I**, D122G	9.6
M7	E7V, H106L, D131G, Q134L, D159E, E170G	7.5
M8	C172S, L277S	6.6
M9	Y214N	4.3[c]
M10	F66L, S121C, D200E	5.2
M11	**Y215H**, Y251C	11.9
M12	I117T, F276Y	7.1
M13	D136V, Q154H, T227S, E271V, D287E	7.0
M14	H198L	7.4
M15	C248Y	5.8
WT	–	3.4
S1	**F108I**, S121C, L277S	44
S2	**Y152F**, E170G, E271V, D287E	20
S3	**F108I**, S121C, D200E, **Y215F**	22
S4	**F108I**, P205H, **Y215H**, E271V	32
S5	**F108I**, V112I, D159E, E170G, S184A, **Y215F**	26
S6	D131G, Q134L, **Y152F**, T227S, Y251C	27
S7	A110G, **Y152F**, Y251C	19
S8	**Y152F**, D159E, E271V	21
F108I	**F108I**	20
Y152F	**Y152F**	20
Y215F	**Y215F**	9.1
Y215H	**Y215H**	13
E271V	E271V	2.9

Mutants M1 to M15 were selected after error-prone PCR; mutants S1 to S8 were selected after DNA shuffling.
[a] Mutations shown in bold are part of the active site. Mutations that are underlined were introduced during gene shuffling.
[b] E-values were determined using 0.5 mM pNPGE as a substrate. The data were fitted to competitive Michaelis-Menten kinetics as described before [26].
[c] Due to enzyme inactivation during the kinetic resolution, no appropriate fit could be obtained. The E-value was calculated from the enantiomeric excess (% e.e.) and percentage of conversion at each point.

proved mutants were subjected to gene shuffling [22]. For this, DNA from these mutants was randomly digested and subsequently reassembled to the full-length *echA* gene. The shuffled DNA was cloned and expressed in *E. coli*. This gave a library of about 20,000 clones, which were screened for activity toward 1,2-epoxybutane using the indicator plate assay. Screening of the resulting 6952 active clones with the pNPGE progress curve analysis method in microtiter plates yielded 86 potentially improved mutants. A further round of testing with cell-free extracts reduced the number to 44 possible candidates, which were used in a kinetic resolution of pNPGE. From this, 8 recombinants were obtained that had a 5.5- to 13-fold improved enantioselectivity toward pNPGE as compared to wild-type (Table 1).

Sequence analysis of the 8 mutants with the largest increase in enantioselectivity showed that 16 of the 34 positions that were present in the EchA mutants obtained by error-prone PCR were maintained in these recombinants (Table 1). Also, two new mutations were introduced during the shuffling procedure (Table 1). Of the total 18 mutated positions, 11 were located in the main domain, all on the C-terminal side of the catalytic nucleophile D107 (Table 1; Figure 3B). The recombina-
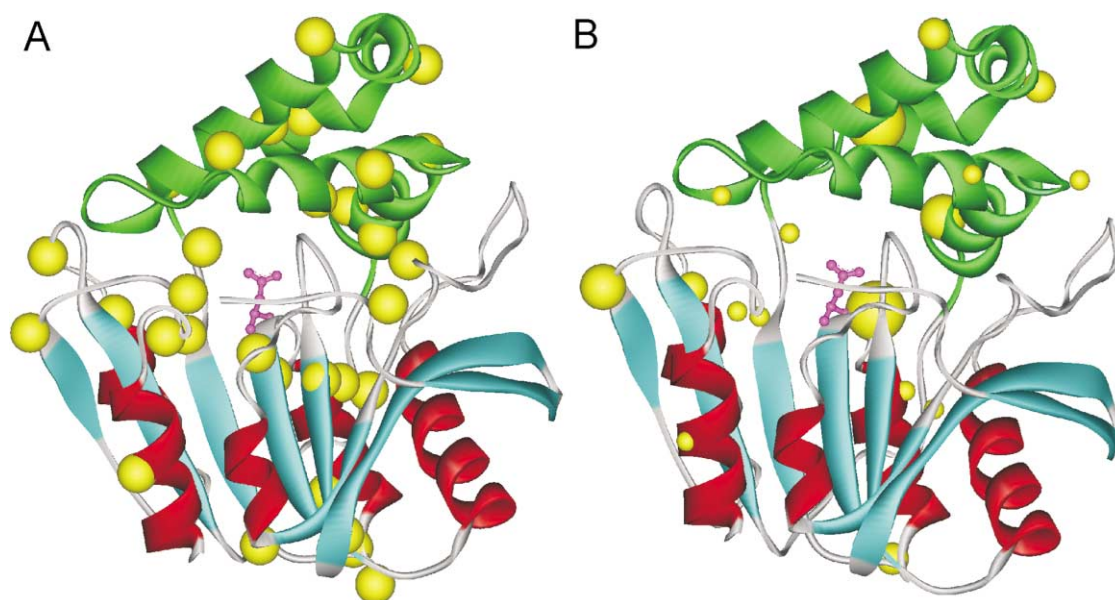
Figure 3. Positions of the Selected Mutations in the X-Ray Structure of EchA

(A), initial mutations selected after error-prone PCR; (B), mutations selected after recombination by gene shuffling. Blue/red, main domain, α/β-hydrolase fold; green, cap domain; purple, active site aspartate; yellow, positions of the mutations. In (B), the radius of the sphere is proportional to the frequency of the mutation in the final set of eight mutants.

tion thus resulted in a focusing of the mutations around the active site of the enzyme (Figure 3B). Indeed, all recombinants contained at least one mutation of a residue that is part of the active site, replacing either one of the tyrosines that is facilitating the epoxide ring opening during the first catalytic step, or replacing F108, which is located next to the catalytic nucleophile.

Characterization of the Improved Recombinants
In order to characterize the recombinant epoxide hydrolases with enhanced enantioselectivity, the enzymes were produced at a larger scale and purified as described before [25]. The recombinant enzymes S1 and S6 appeared unstable during purification and were not further characterized. The other purified mutant enzymes were used to perform kinetic resolutions with seven different racemic epoxides (Figure 1).

The results indicate a remarkable increase in enantioselectivity toward various epoxides besides pNPGE (5), the substrate that was used for screening (Table 2). All mutants had an increased E-value for at least three other substrates. Furthermore, the change in enantioselectivity is largely dependent on the substrate used. The recombinant enzymes containing the mutations in F108 and Y215 all showed a significant increase (2- to 20-fold) in enantioselectivity toward styrene oxide (1) and epichlorohydrin (6). The recombinants containing the Y152F and/or the E271V mutation are significantly enhanced (4- to 8-fold) in their enantioselectivity toward para-nitrostyrene oxide (pNSO, 3) and 1,2-epoxyhexane (7). The most remarkable increase in enantioselectivity was observed for mutant S4, which showed 1.5- to 20-fold improvement of the enantioselectivity toward five compounds besides the selection substrate.

Effect of Single-Site Mutations
In order to determine the effect on enantioselectivity of the most frequently occurring mutations, five single mutants were constructed and their E-values were determined by performing kinetic resolutions (Table 1). All these single mutants, except for mutant E271V, showed an increased enantioselectivity toward pNPGE. The E-values of the shuffled mutants S2, S6, S7, and S8 were similar to that of the Y152F single mutant (Table 1).

The enhanced enantioselectivity of mutant F108I toward pNPGE was mainly due to a lower K_m for the preferred enantiomer, whereas in the wild-type the K_m values for both enantiomers are similar (Table 3). The k_{cat} for both enantiomers has increased as compared to wild-type, but their difference has become somewhat smaller. Mutants S1, S3, S4 and S5 have a higher enantioselectivity toward pNPGE than the single-site F108I mutant (Table 1). Conversion of pNPGE with mutant F108I showed rapid hydrolysis of the (R)-enantiomer as soon as the preferred (S)-enantiomer was completely converted (Figure 4). This unwanted effect is absent in the four shuffling mutants containing this mutation, such as mutant S4 (Table 1; Figure 4). Thus, in this case the additional mutations in the four recombinants have an additional positive effect.

In three of the mutants carrying the F108I substitution, Y215 is also mutated, either to phenylalanine or histidine. When tested separately, it appeared that the single-site mutants Y215F and Y215H also have an increased enantioselectivity toward pNPGE (Table 1). The Y215H mutant showed a large increase in K_m for both enantiomers (Table 3). The resulting k_{cat}/K_m was decreased more for the slower reacting enantiomer than for the preferred (S)-enantiomer, resulting in enhanced enantioselectivity (Table 3). The combination of mutations F108I and

Table 2. The Enantioselectivities of the Purified Improved Mutants toward the Various Epoxides

	Enantioselectivity (E-Value), (Activity[a] (μmol min^{-1} mg^{-1}))						
	1	2	3	4	5	6	7
WT	16 (7.5)	5.7 (1.4)	56 (7.0)	12 (11)	3.4 (12)	<2 (38)	3.6 (7.5)
S2	–[b] (0.6)	–[d] (<0.05)	193 (1.4)	25 (0.06)	20 (2.3)	2.6 (6.5)	23 (4.2)
S3	27 (1.5)	2.3 (1.0)	6.4 (1.3)	17 (0.04)	22 (3.9)	7.5 (18.2)	6.5 (2.8)
S4	>50 (1.4)	4.6 (0.7)	81 (0.6)	15 (0.12)	32 (1.1)	40 (4.2)	27 (3.9)
S5	37 (0.8)	2.3 (0.6)	6.8 (1.0)	3.7 (0.04)	26 (3.1)	7.3 (7.7)	5.5 (2.9)
S7	–[d] (<0.1)	–[d] (<0.05)	>200 (0.6)	18 (0.01)	19 (1.1)	2.6 (2.3)	15 (0.8)
S8	–[c] (0.1)	–[d] (<0.05)	117 (0.6)	13 (0.03)	21 (1.1)	<2 (2.1)	18 (1.5)

Substrate concentrations were 1 mM (epoxide **4**), 2 mM (**2**, **3**, and **5**), or 5 mM (**1**, **6**, and **7**).
[a] Most values were measured at substrates below K_m and therefore do not represent k_{cat} values.
[b] Inactivation occurred during the reaction, resulting in incomplete conversion of the preferred enantiomer, which made the data not suited to determine an accurate E-value.
[c] Activity too low to determine an accurate E-value.
[d] Activity was below the detection limit indicated.

Y215H in mutant S4 and of F108I and Y215F in S3 and S5 resulted in E-values that were higher than those of all single mutants, indicating that also in this case the effect of the mutations was additive (Table 1). In contrast, the enantioselectivity of recombinants S3 and S5 for pNSO was lower than that of the separate F108I and Y215F mutants, whereas recombinant S4 had an E-value between that of the single mutants (Table 3) [5]. Thus, for pNPGE (**5**) the active site mutations were additive, whereas for pNSO they were either antagonistic (S3 and S5) or resulted in the average of the effect of the single-site mutations (S4).

Discussion

In this paper, we show that directed evolution can be used to improve the enantioselectivity of epoxide hydrolase from *A. radiobacter* toward several chiral epoxides. To make it possible to screen large libraries, we used a new agar plate activity detection method for initial selection of clones producing active enzyme. Subsequently, the library of active clones was tested by progress curve analysis for the conversion of the chromogenic substrate pNPGE in microtiter plates. The shape of the progress curves quickly indicates enantioselectivity. This method has the advantage that competitive inhibition of one enantiomer on the conversion of the other, which can be an important factor in enzyme enantioselectivity, is taken into account. Other colorimetric screening methods for improved enantioselectivity used the enantiomers in separate assays, which can provide more accurate information on initial activities [27–29], but may overlook mutants in which the improved enantioselectivity is mainly caused by increased differences between K_m values. The use of a kinetic resolution of pseudo enantiomers followed by ESI-MS analysis also would include this inhibitory effect, since it monitors the kinetic resolution of a (pseudo) racemic mixture [18, 30, 31]. This method was recently used to screen a random mutagenesis library of the epoxide hydrolase from *A. niger* for improved enantioselectivity toward phenyl glycidyl ether [18].

Six of the eight mutants that had an improved enantioselectivity with pNPGE also had enhanced enantioselec-

Table 3. Steady-State Kinetic Parameters and Enantioselectivities of EchA Variants for pNSO (3) and pNPGE (5)

		(R)-pNSO	(S)-pNSO	(R)-pNPGE	(S)-pNPGE
WT	k_{cat} (s^{-1})	2.4	>2.3	3.3	5.3
	K_m (mM)	0.007	>0.5	0.03	0.03
	k_{cat}/K_m (mM^{-1} s^{-1})	343	6.3	110	177
	E-value[a]		54 (56)		1.6 (3.4)
F108I	k_{cat} (s^{-1})	4.5	>2.5	11.2	12.3
	K_m (mM)	0.022	>0.5	0.084	0.0043
	k_{cat}/K_m (mM^{-1} s^{-1})	201	10.5	133	2859
	E-value[b]		19 (15)		22 (20)
Y215H	k_{cat} (s^{-1})	>1.0	>0.006	>0.1	>1.9
	K_m (mM)	>0.1	>0.3	>0.4	>0.7
	k_{cat}/K_m (mM^{-1} s^{-1})	4.6	0.027	0.33	4.1
	E-value[b]		168 (156)		12 (13)
S4	k_{cat} (s^{-1})	>0.27	>0.002	>0.005	>0.56
	K_m (mM)	>0.5	>0.5	>0.25	>0.25
	k_{cat}/K_m (mM^{-1} s^{-1})	0.44	0.005	0.03	1.0
	E-value[b]		88 (81)		33 (32)

For several mutants, only lower limits could be determined for k_{cat}, since the K_m value exceeded the highest substrate concentration that could be used because of low solubility and the strong absorbance of the substrate at high concentrations.
[a] E-values are calculated from the k_{cat}/K_m values for the separate enantiomers. E-values obtained from the kinetic resolution experiments are given in parentheses.
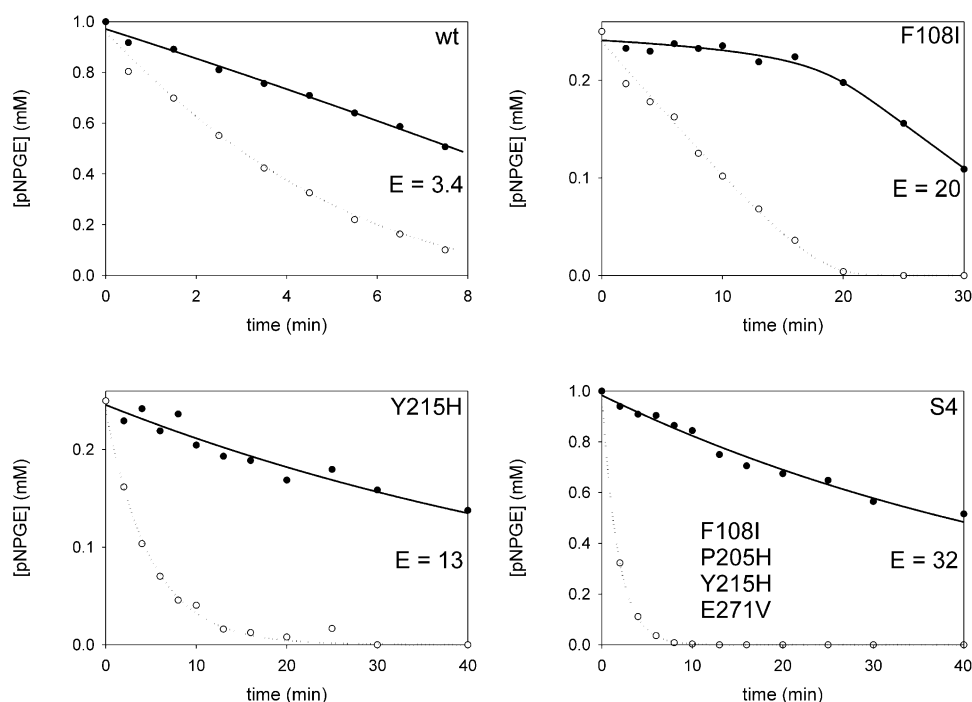
Figure 4. Kinetic Resolutions of pNPGE (5) with Wild-type EchA, Two Site-Directed Mutants, and Recombinant S4

(●), (R)-pNPGE; (○), (S)-pNPGE.

tivities toward other 1,2-epoxides. The substrate pNPGE was chosen for screening, since it gives a spectrophotometric signal during conversion and might mimic 1,2-epoxides with a flexible side group, such as epoxyalkanes or epihalohydrins. Because the highest improvements in enantioselectivity were indeed reached with epichlorohydrin (6) and 1,2-epoxyhexane (7), this approach was apparently working. Few E-values have been reported for other epoxide hydrolases, but they can be calculated from published data on the enantiomeric excess (% e.e.) and yield of the remaining epoxide [32, 33]. When compared with these calculated values, it appeared that the mutants described here have higher enantioselectivity than other enzymes with styrene oxide (1) [32, 33], pNSO (3) [34, 35], phenyl glycidyl ether (4) [18, 32], and epichlorohydrin (6) [32, 33]. For epichlorohydrin, the shuffled mutant S4 has an E-value of 40, which is more than 10-fold higher than the highest enantioselectivity described for this compound so far (E = 3.8, [33]).

In most cases, the enhanced enantioselectivity is due to a reduced k_{cat}/K_m for the nonpreferred enantiomer. Several mutants showed a 2- to 10-fold decrease in conversion rate at the low substrate concentrations that were used (Table 2). This is mainly due to an elevated K_m, since the k_{cat} values were not much reduced for the substrates for which they could be measured (Table 3). Thus, at higher substrate concentrations, which are more practically relevant, the activity will be reduced only a little. The enantioselectivity can improve without significant loss of catalytic rate, since cleavage of the covalent intermediate is the slowest step in the catalytic cycle of A. radiobacter epoxide hydrolase [20]. Enantio-

discrimination is mainly present in the first two steps, which are substrate binding and formation of the covalent intermediate, as was found earlier by pre-steady-state kinetic analysis [20].

In the error-prone PCR mutants, the mutations were mainly present at the interface of the main domain and the cap domain (Figure 3A). The central β sheet of the main domain was free of amino acid substitutions. Mutations in this region that would result in a large change of the side group or introduce a charged group are expected to have a destabilizing effect on the enzyme [36], whereas mutations that cause small changes probably do not alter stereospecificity. Recombination of the beneficial mutations in the DNA shuffling round resulted in focusing of the mutations around the active site and in α helix 3 (amino acids 108–122; Figure 3B). This α helix 3 directly follows the nucleophile elbow, and the mutation could have an effect on the position of the nucleophilic aspartate D107.

In previous studies aimed at improving enantioselectivity of an enzyme, mutations were often found that were located far away from the active site [18, 27–29]. The effects of these mutations were often small as compared to the active site mutations that enhance enantioselectivity we observed in EchA. In all eight shuffled mutants with the highest enantioselectivity, one of the active site residues is mutated. In seven out of these eight shuffled mutants, a mutation occurred in one of the tyrosines that assist in the epoxide ring opening by acting as a proton donor (Table 1). Mutations that replace one of the two tyrosines by a phenylalanine were previously found to enhance enantioselectivity toward a number of aromatic epoxides [5, 17, 19].

Two active site mutations that were not previously found are F108I and Y215H. In mutant Y215H, the histidine probably does not act as a proton donor, since the effect of the mutation on the enantioselectivity and steady-state kinetics of the enzyme for pNSO is similar to that of mutation Y215F (Table 3) [5]. Mutation F108I causes a large improvement in enantioselectivity toward pNPGE, and also the catalytic rate is enhanced. The improved selectivity is based on an increased difference between the K_m values for the enantiomers (Table 3). Previously, a W227F mutation was detected at this conserved position in microsomal epoxide hydrolase and appeared to influence stereoselectivity with glycidyl-4-nitrobenzoate and phenantrene-9,10-oxide [37]. Residue F108 is located next to the active site nucleophile. Its main chain amide is part of the oxyanion hole, and the side group lines the substrate binding site [21]. An altered position of the backbone amide thus is expected to influence rate-limiting hydrolysis of the covalent intermediate, which can explain the observed increase in k_{cat}. The enhanced enantioselectivity is likely due to an interaction between the substrate and the side group of residue 108. In directed evolution studies with lipases, the enhanced enantioselectivity was often due to an altered conformation of the oxyanion hole, resulting in improved conversion [38].

It has been described that combination of mutations can have additive effects in the case of thermostability [39, 40] and enantioselectivity [28, 38]. With the EchA mutants, two pronounced additive effects on enantioselectivity were also found. The kinetic resolution of pNPGE (5) by mutant F108I has the disadvantage that the remaining (R)-enantiomer is rapidly hydrolyzed after the preferred enantiomer is depleted. Fortunately, the introduction of additional mutations overcomes this disadvantage and leads to mutants S3, S4, and S5, in which the remaining enantiomer is only slowly converted (Figure 4), which is due to an elevated K_m and a greatly reduced k_{cat}/K_m for the nonpreferred enantiomer (Table 3). In previous studies, it was shown that mutation Y215F did not improve enantioselectivity toward the aliphatic substrates epichlorohydrin (6) and 1,2-epoxyhexane (7) [17], whereas the combined mutations in S3 and S5 clearly do (Table 2). Thus, directed evolution can rapidly lead to recombinants in which different beneficial mutations that enhance epoxide hydrolase enantioselectivity are combined.

Significance

The enantioselectivity of *Agrobacterium radiobacter* epoxide hydrolase toward *para*-nitrophenyl glycidyl ether (pNPGE) and other epoxides could be improved by using directed evolution. This yielded a range of mutant enzymes with remarkably enhanced potential for the kinetic resolution of epoxides. A rapid and simple agar plate screening was used for activity testing. Spectrophotometric progress curve analysis with a racemic substrate was used to screen for enhanced enantioselectivity. The progress curve analysis method should be generally applicable to other enantioselective reactions that give a chromogenic signal as well.

The enantioselectivity toward aliphatic substrates was especially improved, which reflects the use of pNPGE as a mimic of an aliphatic epoxide substrate. The mutations were focused around the active site of the epoxide hydrolases and mainly affected residues involved in epoxide ring opening. Since this is not the slowest step in the catalytic cycle of the enzyme, enhanced enantioselectivity could be obtained in several mutants without loss of catalytic rate. The results contribute to the development of a toolbox of engineered epoxide hydrolases for use in biocatalysis.

Experimental Procedures

Materials

Safranin O and *para*-nitrophenyl glycidyl ether (pNPGE, epoxide 5 in Figure 1) were purchased from Acros (Geel, Belgium). 1,2-epoxybutane was from Merck. All other epoxides and other chemicals were from Aldrich. All DNA-modifying enzymes and ampicilin were purchased from Roche Molecular Biochemicals, except for *Pwo* DNA polymerase (GENAXIS GmbH), *Pfu* DNA polymerase (Stratagene), and DpnI (New England Biolabs). L-arabinose was from Lancaster (Frankfurt am Main, Germany). All other medium components were from Merck and Difco. Plasmid vector pBAD*myc*HisA and strain *E. coli* TOP10 were from Invitrogen. Oligonucleotides were from Eurosequence BV and Sigma Genosys. The constructs were sequenced at the Biomedical Center in Groningen using the pBAD*myc*HisA forward and reverse primer. The Chiralpak AS, Chiralpak AS-H, and Chiralcel OD HPLC columns were from Diacel Chemical industries. The G-TA capillary GC column was from Astec.

Construction of the Error-Prone PCR Mutant Library

Error-prone PCR of the epoxide hydrolase gene was carried out to construct a mutant library, which could then be screened for enhanced enantioselectivity. The epoxide hydrolase gene from *A. radiobacter* AD1 [25] (*echA*, GenBank accession number Y12804) was cloned downstream of the L-arabinose-inducible *araB* promotor in pBAD*myc*HisA using the forward primer BL035 (5′-GAGCGCGC CATGGCAATTCGACGTCCAGAAGAC-3′) and reverse primer BL036 (5′-GCGCGCCCTGCAGCTAGCGGAAAGCGGTCTTTATTCG-3′). The restriction sites NcoI (forward) and PstI (reverse) that were used are underlined. The pBAD expression system, which we have used previously [41], is more stable than the pGEF-based system that was used by Reetz et al. [18] and Bosma et al. [23]. Error-prone PCR was performed using pBADEchA as a template and 0.4 nM primers BL035 and BL036, 0.2 mM dATP and GTP, 1 mM dCTP and dTTP, and *Taq* buffer containing 5 mM MgCl$_2$ and 0.2 mM MnCl$_2$. *Taq* DNA polymerase was used at a concentration of 0.025 U μl^{-1}. The temperature program used was 4 min at 94°C followed by 30 cycles of 60 s 94°C, 45 s 58°C, and 70 s 72°C and finished with 4 min at 72°C. The PCR product was digested with NcoI and PstI and cloned into NcoI-PstI-digested pBAD*myc*HisA using T4 DNA ligase. The ligation mixture was transformed to *E. coli* TOP10 using electroporation.

Site-Directed Mutagenesis

Site-directed mutants of EchA were made using the QuickChange protocol from Stratagene. Primers used were as follows: F108I sense, 5′-CGTTGGCCATGAtaTCGCGGCCATCG-3′; F108I antisense, 5′-CGATGGCCGCGAtaTCATGGCCAACG-3′; Y215H sense, 5′-GGAGGCTTCAACTACcATCGTGCCAACATAAGG-3′; Y215H antisense: 5′-CCTTATGTTGGCACGAtgGTAGTTGAAGCCTCC-3′; E271V sense, 5′-ACGATGGAGACGATCGtAGACTGCGGTCACTTC-3′; E271V antisense, 5′-GAACTGACCGACGTCTaCGATCGTCTCCATCGT-3′. The mutated codons are in bold, and introduced restriction sites are underlined. Base pair substitutions are in lowercase.

Construction of the Shuffled Library

Plasmid DNA from selected mutants was isolated and used as a template in a normal PCR reaction containing 0.2 mM dNTPs in standard *Pwo* buffer and 0.025 U μl^{-1} *Pwo* DNA polymerase. The

primers and temperature program used were the same as for error-prone PCR. Subsequently, a mixture of equal amounts of each PCR product was treated for 45 s with 1.5 U ml⁻¹ DNase I in order to create fragments of DNA that could then be recombined in a re-assembly PCR. Fragments ranging from 100–250 bp were isolated from a 2% agarose gel and subjected to a reassembly PCR without primers, using 0.4 mM dNTPs and *Pwo* DNA polymerase. The temperature program used was 30 s at 94°C, followed by 60 cycles of 60 s at 94°C, 45 s 58°C, 70 s 72°C, and finished by 10 min at 72°C. Reassembled DNA of around 0.9 kb was isolated from a 0.8% agarose gel and used as a template in a normal PCR reaction in order to restore the restriction sites in all reassembled fragments. The reassembled genes were cloned into pBAD*myc*HisA and transformed to *E. coli* by electroporation.

Agar Plate Assay for Epoxide Hydrolase Activity
Transformed cells were put on agar plates containing 6 g l⁻¹ trypton, 3 g l⁻¹ yeast extract, 10 g l⁻¹ NaCl, 50 μg ml⁻¹ ampicilin, 0.02% (w/v) L-arabinose, and 100 μM safranin O. Cells were grown overnight at 30°C, followed by overnight incubation at room temperature. The plates were subsequently placed in a closed jar and exposed to 1,2-epoxybutane vapor for 9 hr at room temperature and then incubated overnight at room temperature in order to allow the cells to generate excess NADH by oxidation of the vicinal diol formed as a result of epoxide hydrolysis. Inactive colonies had an unstained outer ring, whereas active colonies appeared as homogeneously purple colonies. The positive colonies were used to inoculate 200 μl Luria-Bertani (LB) medium with 10% (v/v) glycerol in 96-well plates. The inoculated plates were grown overnight at 30°C and stored at −80°C. Expression of the mutant enzymes was achieved by duplicating the storage library in 96-well plates containing LB medium with 0.02% (w/v) L-arabinose, followed by overnight growth at 30°C. In all media, ampicillin was used at a concentration of 50 μg ml⁻¹.

Screening for Improved Enantioselectivity Using Spectrophotometric Progress Curve Analysis
The E-value of a kinetic resolution can be estimated from the shape of a progress curve in which conversion of a racemic substrate is plotted against time. With low enantioselectivity, conversion can be followed to completion (curve with E = 3.4 in Figure 2C). If the conversion is perfectly enantioselective, a progress curve will display incomplete hydrolysis and the reaction stops at 50% conversion (see simulated curve with E = 500 in Figure 2C). If enantioselectivity is modest, two distinct kinetic phases are obtained, with a bend in the curve at around 50%–60% conversion, which is the result of the difference between the kinetic parameters of the enzyme for the two enantiomers (curve with E = 32 in Figure 2C). If a colorimetric substrate is used, a progress curve can be recorded using a spectrophotometer, and the resulting curve is governed by the following equation, which can be numerically integrated over time:

$$\frac{dA}{dt} = (\epsilon_{diol} - \epsilon_{epox}) * \left(\frac{k_{catS}*Enz*S}{S + \left(\frac{R}{K_{mR}} + 1\right)*K_{mS}} + \frac{k_{catR}*Enz*R}{R + \left(\frac{S}{K_{mS}} + 1\right)*K_{mR}} \right).$$

The position of the bend and the initial and final rate of conversion provide information about the enantioselectivity and kinetic properties of the enzyme. To screen a large number of mutants for improved enantioselective behavior, a progress curve of the conversion of *para*-nitrophenyl glycidyl ether (pNPGE, epoxide 5 in Figure 1) for each mutant was recorded in a microtiter plate reader at 350 nm ($\epsilon_{350epoxide}$ = 3993 M⁻¹ cm⁻¹, $\epsilon_{350diol}$ = 4572 M⁻¹ cm⁻¹). The initial rate (V_{init}) and the final rate (V_{term}) as well as the A_{350} at t = 0 and t = 60 min were scored and used for evaluation. Progress curves showing a high V_{init}:V_{term} ratio, combined with incomplete conversion of the substrate, were expected to be biphasic and were inspected for the presence of two distinct kinetic phases.

Cell-free extracts made from cultures that were selected as candidates with possibly improved enantioselectivity were used for measuring progress curves at 350 nm in a normal cuvette. The measurements were done in 100 mM Tris-SO₄ (pH 9.0) at 30°C on a Perkin Elmer Lambda Bio 10 UV/VIS spectrophotometer. The substrate was added from a stock solution of 25–50 mM in dimethyl sulfoxide

(DMSO) to a final concentration between 0.2 and 0.5 mM. The final concentration of DMSO was less than 1% (v/v). A suitable amount of cell-free extract (CFE) was added to start the reaction. The resulting curves were inspected for biphasic behavior, and the mutants that were confirmed to be positive were selected for the next step in the screening procedure.

Spectrophotometric Epoxide Hydrolase Assays
Steady-state kinetic parameters of purified wild-type and mutant epoxide hydrolases were determined by measuring progress curves of the conversion of enantiopure *para*-nitrostyrene oxide (pNSO, 3) and pNPGE (5). Substrate was added up to a concentration of 0.5 mM with a final concentration of DMSO lower than 1% (v/v). A suitable amount of purified protein was added to start the reaction. These measurements were performed on a Kontron Uvikon 930 UV/VIS spectrophotometer. The spectrophotometric substrate conversion traces for the separate enantiomers of 3 were directly fitted to Michaelis-Menten kinetics as described before [5]. The traces for both enantiomers of 5 were fitted in a similar fashion using the extinction coefficients for epoxide 5 (ϵ_{350}= 3993 M⁻¹ cm⁻¹) and the corresponding vicinal diol (ϵ_{350}= 4572 M⁻¹ cm⁻¹).

Kinetic Resolutions
The enantioselectivity of the mutants for various epoxides (Figure 1) was determined by performing a kinetic resolution of 0.5–5 mM of racemic substrate in 8–20 ml of 100 mM Tris-SO₄ (pH 9.0). The reaction was started by adding a suitable amount of CFE or purified enzyme, and samples were taken in time and extracted with hexane or ether containing an internal standard. If ether was used for extraction, the samples were dried on a short column of anhydrous MgSO₄. The samples were analyzed using chiral HPLC and GC. The data were fitted to competitive Michaelis-Menten kinetics as described before [26] in order to determine the E-value.

Chiral HPLC and GC Analysis
For the analysis of the conversion of epoxides 1, 2, 6, and 7 (Figure 1), a Chiraldex G-TA capillary GC column was used and mesitylene or 1-chlorohexane was used as an internal standard. Epoxide 1: mesitylene, t_r = 3.0 min; (S)-1, t_r = 5.2 min; (R)-1, t_r = 5.9 min at 110°C. Epoxide 2: mesitylene, t_r = 2.2 min; (S)-2, t_r = 8.0 min; (R)-2, t_r = 9.9 min with 7 min at 120°C; 5°C min⁻¹ to 150°C. Epoxide 6: 1-chlorohexane, t_r = 3.0 min; (S)-6, t_r = 3.2 min; (R)-6, t_r = 3.4 min at 80°C. Epoxide 7: (S)-7, t_r = 5.7 min; (R)-7, t_r = 6.0 min; mesitylene, t_r = 10.1 min at 60°C. The conversion of epoxides 3, 4, and 5 (Figure 1) was analyzed using various chiral HPLC columns with mesitylene or *para*-nitroacetophenone as an internal standard. Epoxide 3: mesitylene, t_r = 3.0 min; (R)-3, t_r = 9.2 min; (S)-3, t_r = 12.6 min on a Chiralpak AS-H column with heptane:2-propanol 7:3 as the eluent. Epoxide 4: mesitylene, t_r = 3.1 min; (R)-4, t_r = 6.1 min; (S)-4, t_r = 9.3 min on a Chiralcel OD column with heptane:2-propanol 4:1 as the eluent. Epoxide 5: *para*-nitroacetophenone, t_r = 10.0 min; (S)-5, t_r = 23.2 min; (R)-5, t_r = 27.6 min on a Chiralpak AS column with heptane:2-propanol 7:3 as the eluent. With all HPLC separations, the flow rate was 1.0 ml min⁻¹.

Protein Expression and Purification
Expression of EchA mutants was achieved by inoculating 3 liters of LB medium containing 0.02% L-arabinose and 50 μg ml⁻¹ ampicilin with a 250 ml preculture without L-arabinose. The induced cells were grown overnight at room temperature. The cells were centrifuged and washed in 250 ml TEMAG (pH 7.5) at 4°C. A cell-free extract was made, and the protein was purified using DEAE-52 Sepharose anion exchange chromatography followed by a hydroxyapatite step, as described before [25].

Preparation of Epoxides
Epoxide 2 was synthesized from *meta*-chlorobenzaldehyde in the same way as *para*-chlorostyrene oxide was previously synthesized from *para*-chlorobenzaldehyde [26]. The racemate of epoxide 3 was synthesized as described before [42]. (R)-3 and (S)-3 were obtained by HPLC separation on a Chiralpak AS preparative column. (R)-5 and (S)-5 were synthesized from *para*-nitrophenol and (R)- or (S)-

glycidyl-3-nitrobenzene sulfonate, respectively, according to a procedure described before [43].

References

1. Arand, M., Hallberg, B.M., Zou, J., Bergfors, T., Oesch, F., van der Werf, M., de Bont, J.A.M., Jones, T.A., and Mowbray, S.L. (2003). Structure of *Rhodococcus erythropolis* limone-1,2-epoxide hydrolase reveals a novel active site. EMBO J. *22*, 2583–2592.

2. Ollis, D.L., Cheah, E., Cygler, M., Dijkstra, B., Frolow, F., Franken, S.M., Harel, M., Remington, S.J., Silman, I., Schrag, J., et al. (1992). The α/β hydrolase fold. Protein Eng. *5*, 197–211.

3. Arand, M., Grant, D.F., Beetham, J.K., Friedberg, T., Oesch, F., and Hammock, B.D. (1994). Sequence similarity of mammalian epoxide hydrolases to the bacterial haloalkane dehalogenase and other related proteins. Implication for the potential catalytic mechanism of enzymatic epoxide hydrolysis. FEBS Lett. *338*, 251–256.

4. Argiriadi, M.A., Morisseau, C., Goodrow, M.H., Dowdy, D.L., Hammock, B.D., and Christianson, D.W. (2000). Binding of alkylurea inhibitors to epoxide hydrolase implicates active site tyrosines in substrate activation. J. Biol. Chem. *275*, 15265–15270.

5. Rink, R., Lutje Spelberg, J.H., Pieters, R.J., Kingma, J., Nardini, M., Kellogg, R.M., Dijkstra, B.W., and Janssen, D.B. (1999). Mutation of tyrosine residues involved in the alkylation half reaction of epoxide hydrolase from *Agrobacterium radiobacter* AD1 results in improved enantioselectivity. J. Am. Chem. Soc. *121*, 7417–7418.

6. Rink, R., Kingma, J., Lutje Spelberg, J.H., and Janssen, D.B. (2000). Tyrosine residues serve as proton donor in the catalytic mechanism of epoxide hydrolase from *Agrobacterium radiobacter*. Biochemistry *39*, 5600–5613.

7. Bloom, J.D., Dutia, M.D., Johnson, B.D., Wissner, A., Burns, M.G., Largis, E.E., Dolan, J.A., and Claus, T.H. (1992). Disodium (*R,R*)-5-[2-[[2-(3-chlorophenyl)-2-hydroxylethyl]-amino]propyl]-1,3-benzodioxole-2,2-dicarboxylate (CL316,243). A potent β-adrenergic agonist virtually specific for β_3-receptors. A promising antidiabetic and antiobesity agent. J. Med. Chem. *35*, 3081–3084.

8. Pfeiffer, F.R., Wilson, J.W., Weinstock, J., Kuo, G.Y., Chambers, P.A., Holden, K., Hahn, G., Wardell Jr, R.A., Jr., Tobia, A.J., Setler, P.E., et al. (1982). Dopaminergic activity of substituted 6-chloro-1-phenyl-2,3,4,5-tetrahydro-1*H*-3-benzazepines. J. Med. Chem. *25*, 352–358.

9. Hett, R., Fang, Q.K., Gao, Y., Hong, Y., Butler, H.T., Nie, X., and Wald, S.A. (1997). Enantio- and diastereoselective synthesis of all four stereoisomers of formoterol. Tetrahedron Lett. *38*, 1125–1128.

10. Kabat, M.M., Daniewski, A.R., and Burger, W. (1997). A convenient synthesis of *R*-(-)-carnitine from *R*-(-)-epichlorohydrin. Tetrahedron Asymmetry *8*, 2663–2665.

11. Schaus, S.E., and Jacobsen, E.C. (1996). Dynamic kinetic resolution of epichlorohydrin via enantioselective catalytic ring opening with TMSN$_3$. Practical synthesis of aryl oxazolidinone antibacterial agents. Tetrahedron Lett. *37*, 7937–7940.

12. Takano, S., Kamikubo, T., Sugihara, T., Suzuki, M., and Ogasawara, K. (1993). Enantioconvergent synthesis of a promising HMG Co-A reductase inhibitor NK-104 from both enantiomers of epichlorohydrin. Tetrahedron Asymmetry *4*, 201–204.

13. Katsuki, T. (2002). Chiral metallosalen complexes: structures and catalysts tuning for asymmetric epoxidation and cyclopropanation. Adv. Synth. Catal. *344*, 131–147.

14. Panke, S., Wubbolts, M.G., Schmid, A., and Witholt, B. (2000). Production of enantiopure styrene oxide by recombinant *Escherichia coli* synthesizing a two-component styrene monooxygenase. Biotechnol. Bioeng. *69*, 91–100.

15. Tokunaga, M., Larrow, J.F., Kakiuchi, F., and Jacobsen, E.N. (1997). Asymmetric catalysis with water: efficient kinetic resolution of terminal epoxides by means of catalytic hydrolysis. Science *277*, 936–938.

16. Archelas, A., and Furstoss, R. (2001). Synthetic applications of epoxide hydrolases. Curr. Opin. Chem. Biol. *5*, 112–119.

17. Lutje Spelberg, J.H., Rink, R., Archelas, A., Furstoss, R., and Janssen, D.B. (2002). Biocatalytic potential of the epoxide hydrolase from *Agrobacterium radiobacter* AD1 and a mutant with enhanced enantioselectivity. Adv. Synth. Catal. *344*, 980–985.

18. Reetz, M.T., Torre, C., Eipper, A., Lohmer, R., Hermes, M., Brunner, B., Maichele, A., Bocola, M., Arand, M., Cronin, A., et al. (2004). Enhancing enantioselectivity of an epoxide hydrolase by directed evolution. Org. Lett. *6*, 177–180.

19. Genzel, Y., Archelas, A., Lutje Spelberg, J.H., Janssen, D.B., and Furstoss, R. (2001). Microbiological transformations. Part 48: Enantioselective biohydrolysis of 2-, 3- and 4-pyridyloxirane at high substrate concentration using the *Agrobacterium radiobacter* AD1 epoxide hydrolase and its Tyr215Phe mutant. Tetrahedron *57*, 2775–2779.

20. Rink, R., and Janssen, D.B. (1998). Kinetic mechanism of the enantioselective conversion of styrene oxide by epoxide hydrolase from *Agrobacterium radiobacter* AD1. Biochemistry *37*, 18119–18127.

21. Nardini, M., Ridder, I.S., Rozeboom, H.J., Kalk, K.H., Rink, R., Janssen, D.B., and Dijkstra, B.W. (1999). The X-ray structure of epoxide hydrolase from *Agrobacterium radiobacter* AD1. An enzyme to detoxify harmful epoxides. J. Biol. Chem. *274*, 14579–14586.

22. Stemmer, W.P. (1994). Rapid evolution of a protein in vitro by DNA shuffling. Nature *370*, 389–391.

23. Bosma, T., Damborsky, J., Stucki, G., and Janssen, D.B. (2002). Biodegradation of 1,2,3-trichloropropane through directed evolution and heterologous expression of a haloalkane dehalogenase gene. Appl. Environ. Microbiol. *68*, 3582–3587.

24. Zannotti, A., and Azzone, G.F. (1980). Safranine as mebrane potential probe in rat liver mitochondria. Arch. Biochem. Biophys. *201*, 255–265.

25. Rink, R., Fennema, M., Smids, M., Dehmel, U., and Janssen, D.B. (1997). Primary structure and catalytic mechanism of the epoxide hydrolase from *Agrobacterium radiobacter* AD1. J. Biol. Chem. *272*, 14650–14657.

26. Lutje Spelberg, J.H., Rink, R., Kellogg, R.M., and Janssen, D.B. (1998). Enantioselectivity of a recombinant epoxide hydrolase from *Agrobacterium radiobacter*. Tetrahedron Asymmetry *9*, 459–466.

27. Reetz, M.T., Wilensek, S., Zha, D., and Jaeger, K.-E. (2001). Directed evolution of an enantioselective enzyme trough combinatorial multiple cassette mutagenesis. Angew. Chem. Int. Ed. Engl. *40*, 3589–3591.

28. Liebeton, K., Zonta, A., Schimossek, K., Nardini, M., Lang, D., Dijkstra, B.W., Reetz, M.T., and Jaeger, K.E. (2000). Directed evolution of an enantioselective lipase. Chem. Biol. *7*, 709–718.

29. Zha, D., Wilensek, S., Hermes, M., Jaeger, K.-E., and Reetz, M.T. (2003). Complete reversal of enantioselectivity of an enzyme-catalyzed reaction by directed evolution. Chem. Commun., 2664–2665.

30. Reetz, M.T., Becker, M.H., Klein, H.-W., and Stöckigt, D. (1999). A method for high-throughput screening of enantioselective catalysts. Angew. Chem. Int. Ed. Engl. *38*, 1758–1761.

31. Schrader, W., Eipper, A., Pugh, D.J., and Reetz, M.T. (2002). Second-generation MS-based high-throughput screening systems for enantioselective catalysts and biocatalysts. Can. J. Chem. *80*, 626–636.

32. Choi, W.J., Huh, E.C., Park, H.J., Lee, E.Y., and Choi, C.Y. (1998). Kinetic resolution for optically active epoxides by microbial enantioselective hydrolysis. Biotechnol. Tech. *12*, 225–228.

33. Weijers, C.A.G.M. (1997). Enantioselective hydrolysis of aryl, alicyclic and aliphatic epoxides by *Rhodoturola glutinis*. Tetrahedron Asymmetry *8*, 639–647.

34. Nellaiah, H., Morisseau, C., Archelas, A., Furstoss, R., and Baratti Jacques, C. (1996). Enantioselective hydrolysis of *p*-nitrostyrene oxide by an epoxide hydrolase preparation from *Aspergillus niger*. Biotechnol. Bioeng. *49*, 70–77.

35. Morisseau, C., Nellaiah, H., Archelas, A., Furstoss, R., and Baratti Jacques, C. (1997). Asymmetric hydrolysis of racemic *para*-nitrostyrene oxide using an epoxide hydrolase preparation from *Aspergillus niger*. Enzyme Microb. Technol. *20*, 446–452.

36. Merkel, J.S., Sturtevant, J.M., and Regan, L. (1999). Sidechain interactions in parallel β sheets: the energetics of cross-strand pairings. Structure *7*, 1333–1343.

37. Laughlin, L.T., Tzeng, H.F., Lin, S., and Armstrong, R.N. (1998). Mechanism of microsomal epoxide hydrolase. Semifunctional site-specific mutants affecting the alkylation half-reaction. Biochemistry *37*, 2897–2904.

38. Bocola, M., Otte, N., Jaeger, K.-E., Reetz, M.T., and Thiel, W. (2004). Learning from directed evolution: theoretical investigations into cooperative mutations in lipase enantioselectivity. Chembiochem *5*, 214–223.

39. Hoseki, J., Okamoto, A., Takada, N., Suenaga, A., Futatsugi, N., Konagaya, A., Taiji, M., Yano, T., Kuramitsu, S., and Kagamiyama, H. (2003). Increased rigidity of domain structures enhances the stability of a mutant enzyme created by directed evolution. Biochemistry *42*, 14469–14475.

40. Lehmann, M., Loch, C., Middendorf, A., Studer, D., Lassen, S.F., Pasamontes, L., van Loon, A.P.G.M., and Wyss, M. (2002). The consensus concept for thermostability engineering of proteins: further proof of concept. Protein Eng. *15*, 403–411.

41. Pikkemaat, M.G., and Janssen, D.B. (2002). Generating segmental mutations in haloalkane dehalogenase: a novel part in the directed evolution toolbox. Nucleic Acids Res. *30*, E35.

42. Westkaemper, R.B., and Hanzlik, R.P. (1981). Mechanistic studies of epoxide hydrolase utilizing a continuous spectrophotometric assay. Arch. Biochem. Biophys. *208*, 195–204.

43. Kitaori, K., Furukawa, Y., Yoshimoto, H., and Otera, J. (1999). CsF in organic synthesis. Regioselective nucleophilic reactions of phenols with oxiranes leading to enantiopure β-blockers. Tetrahedron *55*, 14381–14390.